buildings

MDPI

Article

Modeling of an Aerogel-Based "Thermal Break" for Super-Insulated Window Frames

Alessandro Cannavale [1,2,*], Francesco Martellotta [1], Umberto Berardi [3], Chiara Rubino [1], Stefania Liuzzi [1], Vincenzo De Carlo [4] and Ubaldo Ayr [1]

1 Department of Civil Engineering and Architecture (DICAR), Technical University of Bari, via Orabona 4, 70125 Bari, Italy; francesco.martellotta@poliba.it (F.M.); chiara.rubino@poliba.it (C.R.); stefania.liuzzi@poliba.it (S.L.); Ubaldo.Ayr@poliba.it (U.A.)
2 Istituto di Nanotecnologia, CNR Nanotec, Via Arnesano 16, 73100 Lecce, Italy
3 Department of Architectural Science, Ryerson University, 350 Victoria St., Toronto, ON M5B 2K3, Canada; uberardi@ryerson.ca
4 Dcs Group S.R.L., Via per Castellaneta Z. Ind. S. Basilio, 74017 Mottola (Ta), Italy; vincenzo.decarlo@decarlo.it
* Correspondence: alessandro.cannavale@poliba.it; Tel.: +39-080-5963718

Received: 7 February 2020; Accepted: 12 March 2020; Published: 18 March 2020

Abstract: Research activities in the field of innovative fixtures are continuously aiming at increasing their thermal and optical performances to offer optimal exploitation of daylight and solar gains, providing effective climate screen, according to increasing standards for indoor comfort and energy saving. Within this work, we designed an innovative aerogel-based "thermal break" for window frames, so as to consistently reduce the frame conductance. Then, we compared the performance of this new frame both with currently used and obsolete frames, present in most of the existing building stock. Energy savings for heating and cooling were assessed for different locations and confirmed the potential role played by super-insulating materials in fixtures for extremely rigid climates.

Keywords: window frame; granular aerogel; energy saving

1. Introduction

Awareness of the anthropogenic effects on the environment dramatically has increased in recent years, especially in terms of global warming and uncontrolled greenhouse gas production. For this reason, the control of energy consumption of buildings is a pivotal challenge. The latest European Directive 2018/844 reports that the building stock contributes to 36% of greenhouse gas emissions, considering that almost 50% of the Union's final energy consumption is used for heating and cooling, and 80% of this amount is employed in buildings [1]. The 2015 Paris Agreement on climate change, following the United Nations Conference on Climate Change (COP21), required the subscribing States to reduce carbon emissions in the building stock. To do this, in the EU and worldwide, the priority is to enhance energy efficiency by deploying low-cost renewable energies and innovative technologies, especially deriving from recent achievements in the field of nanomaterials research, with reference to building integration of novel technologies, spanning from chromogenics [2] to semi-transparent photovoltaics [3,4], super-insulating materials [5,6], and phase change materials [7,8]. One of the possible approaches, especially in countries with a more rigid climate, is to find new devices to increase the standards of insulation of buildings. This challenge can be taken up by some materials, defined as super-insulators [5], characterized by a relatively lower thermal conductivity compared with the typical insulating materials used in building envelopes. The main evaluation parameters in the choice of an innovative insulating material are undoubtedly the thermal conductivity, but also volume and

cost [9–11]. For these reasons, interest in a nanostructured porous material called aerogel has been growing in recent years [12,13]. The name itself, aerogel, indicates a precise property of the material, namely, the substitution of the liquid component of the gel with a gas. The gel is generally made by means of low temperature sol–gel technique.

1.1. Aerogel for Super-Insulation

The synthesis of the aerogel involves the hydrolysis and condensation at room temperature of a solution, starting from an alkoxide precursor (tetraethyl-orthosilicate, tetramethyl orthosilicate, or poly-ethoxydisiloxane are the most used), in the presence of a convenient catalyst [5]. A continuous three-dimensional lattice forms inside the liquid. After the aging phase of the gel and the subsequent removal of water from the inside of the pores with solvent washes, the material is ready for the drying process. Although there are different ways to proceed with the drying of the silica gel, the most widespread is still the so-called supercritical drying method. The substitution gives rise to a structure made of silica gel containing pores with a diameter of variable size (between 5 and 70 nm) and a density between 70 and 150 kg/m^3 [14]. For this reason, aerogel can be considered an open-celled, mesoporous solid foam containing a network of nanostructures.

The resulting material is characterized by a thermal conductivity that can be very low (0.013 W/m·K) [15], in which the nanopores occupy more than 85% of the volume; the high porosity allows the obtaining of interesting properties from the optical, thermal, and physical point of view [16]. The very low thermal conductivity of the aerogel is due to the very small fraction of solid silica: the structure skeleton contains a large number of free ends that "complicate" the path of the thermal flow. The size of pores (~20 nm) hinders thermal conduction, which is inversely proportional to the diameter of the pores themselves. Moreover, the dimension of the pores prevents the Brownian motion of the air molecules and therefore prevents convective heat exchange [17]. As stated by Baetens [11], if one would be able to find a cheaper manufacturing process, aerogel might become a real alternative to existing building insulating materials.

1.2. Aerogel Products for Constructions

Currently, aerogel products are available for construction as monolithic panels with high transparency [18], small size granules [19,20], or thermal insulation blankets [21,22]. Each of these products can be employed to improve the thermal performance of mortars and concretes; plasters for opaque systems [16,23]; or translucent/transparent systems, such as insulating glazed units, suitably filled with monolithic or granular aerogels [10,24,25]. In terms of potential aerogel applications, windows represent the best candidates because they are a thermal "weak point" in the building envelope, due to their relatively higher global heat exchange coefficient compared to opaque surfaces.

1.3. Aerogel Insulation for Windows

Aerogel can be used in windows in various ways, as reported in the literature [26]. If aerogel were used to fill air gaps between glass panes, the consequent benefits would be represented by lower solar heat gain coefficient, as glazing containing aerogel is translucent and lower values of glazing thermal transmittance (U_g) would be obtained. Double- or triple-glazed units filled with aerogel—as granules or in a monolithic form—will output a diffuse light, which is sometimes desirable to achieve comfort in large commercial or office spaces, airports, museums, etc. However, it is in terms of reduction in energy consumption that aerogel may make a difference compared to conventional materials. It has been proven that granular aerogel may reduce the heat loss in office buildings [27] by 80% or cooling load in humid subtropical climates by 4% [28]. A study by Gao et al. also reported a yearly saving as high as 21% in a building's energy consumption [29]. Moretti and Buratti compared monolithic aerogel glass panes to conventional glazing systems, reporting a 55% reduction in heat losses, whereas granular aerogel windows showed a 25% reduction in heat losses. In the latter case, a 66% reduction in visible transmittance was observed [30,31]. A recent work investigated the effect of inserting an aerogel

blanket in the air chambers of a PVC window frame, leading to a reduction in the frame U-value from 1.06 to 0.92 W/m^2·K [32]. In the present work, the energy benefits achievable by using granular aerogel inside the fixed and mobile frames of a high thermal performance window were studied. The window frame was made of wood and aluminium and an interposed aerogel thermal break was also used. A finite element method analysis of a window frame containing aerogel was carried out, obtaining a high performance level. This innovative window was compared with others, embodying different frames, as explained in the Methodology section, by means of simulations in test rooms within the Energyplus software platform [33]. Energy consumption for heating and cooling was tested within a typical office on all possible exposures, in two locations with very different climates: the Canadian city of Toronto and Bari, in Southern Italy.

2. Materials and Methods

2.1. Frame and Window Description

This innovative window (Figure 1), specifically designed to meet the highest thermal insulation standards, includes a three-pane glazing. The internal glazing embodied a low emittance coating (ε = 0.21) deposited on face 5, i.e., the outer face of the internal pane. The aerogel section (the red part in Figure 2) was conveniently surrounded by a thin acrylonitrile–butadienestyrene (ABS) skin (2 mm thick), and embodied granular aerogel within the frame section, thus behaving like a super-insulating "thermal break", between the external aluminium frame and the internal wooden frame. The same ABS skin is generally adopted in existing commercial frames using the same technology, to embody expanded polystyrene (Isover EPS 035) insulating material. Cabot Enova IC3100 granular aerogel was used, with granule size spanning between 2 and 40 µm, a thermal conductivity of 0.012 W/m·K at ambient temperature, and very low density, ranging from 120 to 150 kg/m^3 according to technical specifications of the material. The coupling between the aerogel section and the wooden frame was made by using a stripe of aerogel blanket, Pyrogel-XTE by Aspen, with comparable thermal conductivity (less than 0,02 W/m·K) suitably glued and mechanically fixed to the frame.

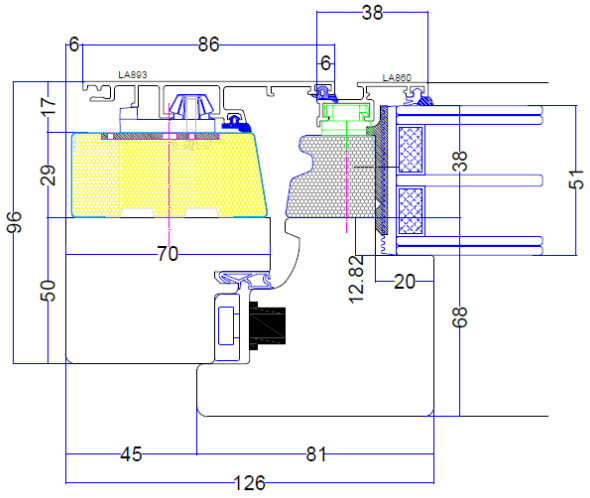

Figure 1. Cross section of the frame reporting dimensional data of the reference window frame, corresponding to a window designed in compliance with regulations. Above, the external aluminum section is clearly visible; in the intermediate part, the area devoted to thermal insulation (in yellow); below, the wooden profile, facing the indoor space.

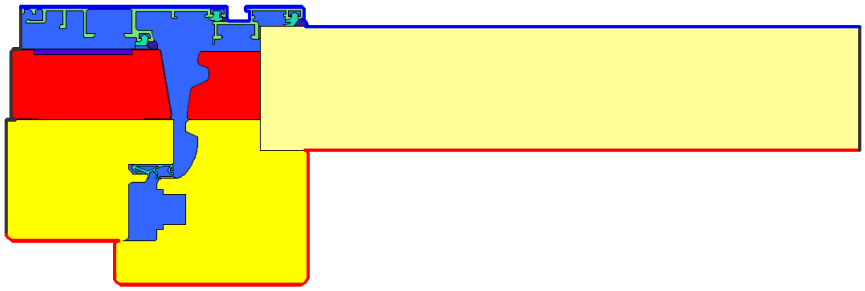

Figure 2. Cross section of the frame, as designed in the finite element method software Flixo, used for the simulation. In this case, each color represents a material, modeled with different thermal properties. The yellow section on the left represents soft wood; the light yellow area represents the replacement panel with given thermal resistance, replacing the triple glass in the numerical analysis; the aerogel is colored in red; and the aluminium is in light green. A different shade of green was used for EPDM and light blue for air within the frame.

2.2. Finite Element Method

The thermal heat loss due to the transmission through windows is strongly affected by the technical features of their transparent (glazing) and opaque (frames and spacers) components. Such figure of merit can be determined according to the standard ISO 10077-2:2017, "Thermal performance of windows, doors and shutters—Part 2: Numerical method of frames" [34]. To calculate the thermal transmittance for the two-dimensional window section, including the frame and the glazing, according to the standard, the thermal transmittance of the frame section (U_f) in W/m^2·K must be calculated according to the following formula, remembering that in the computational model, glazing must be replaced with a panel with given thermal insulating properties,

$$U_f = \frac{L_{\mathrm{f}}^{2D} - U_p b_p}{b_f} \tag{1}$$

where U_p is the thermal transmittance of the replacement panel, in W/m^2·K, which is assumed to have a thermal conductivity of 0.035 W/m·K, according to EN ISO 10077-2; b_{f} is the width of the frame section in m; and b_p is the visible width of the panel, in m. $L_{\mathrm{f}}{}^{2D}$ is the thermal conductance of the section in W/m·K, calculated from the total heat flow rate per unit length through the section divided by the temperature difference between both adjacent environments. The value of U_f, according to current standards, was obtained by using the commercial software Flixo, allowing CAD-based input of constructions and to import DXF-files and materials databases, to make a detailed two-dimensional finite elements analysis of the frame, in steady-state conditions (Figure 2).

Afterwards, the global thermal exchange coefficient of the whole window (U_w) was calculated according to the equation reported in the standard ISO 10077-1:2017, "Thermal performance of windows, doors, and shutters—Calculation of thermal transmittance—Part 1: General" [34]:

$$U_w = \frac{A_g U_g + A_f U_f + \Psi_g l_g}{A_g + A_f} \tag{2}$$

where U_g is the thermal transmittance of the glass section (W/m^2·K); A_g and A_f are the surface areas of glazing and frame, respectively (m^2); Ψ_g is the linear thermal transmittance of the glazing joint (W/m·K); and l_g is its length (m), calculated according to ISO 10077-2.

To highlight the effect of the aerogel material, further FEM simulations were made to compare the thermal performance of the aerogel-based frame with those observed in a similar frame, embodying expanded polystyrene, instead of granular aerogel. Other materials used in this FEM analysis (Figure 2) were aluminium (λ = 160 W/m·K), ethylene propylene diene monomer (EPDM, with λ = 0.25 W/m·K),

soft wood (λ = 0.12 W/m·K), Cabot 3120 granular aerogel (λ = 0.012 W/m·K), and expanded polystyrene (λ = 0.035 W/m·K).

The innovative window has been fabricated, and some images of the designed prototype are shown in Figure 3. Experimental campaigns will subsequently be carried out in order to assess the energy saving benefits obtainable with this type of window frame, in the context of a real building.

Figure 3. Aerogel-enhanced window (Aeroshield) embodying a triple-glazed unit, with external aluminium frame and internal wooden frame (**a**); Reference frame with expanded polystyrene insulation, in black (b); Aerogel-insulated frame with polymer skin (**c**).

2.3. EnergyPlus Model

To analyze the energy performance implications, the aerogel-based window was compared to different window configurations. The first one, identified as "Standard compliant scenario", was made of an aluminium frame with the so-called "thermal break", i.e., a continuous polymer barrier between internal and external parts of window frames, preventing conductive thermal energy loss and a triple-glazed unit with the same properties of the newly designed window, so as to assess performance benefits strictly deriving from the use of aerogel in frames. The second kind of window considered was made of an obsolete double-glazed unit and a simple aluminium frame, with no thermal break inside. The latter window was considered to envisage results in a "Refurbishment scenario", a useful comparison with typical window performance in the existing building stock.

A 3D geometrical model of the case study was first designed in SketchUp, using the OpenStudio plugin. Afterwards, it was imported in EnergyPlus v. 8.9, a free simulation tool by the U.S. Department of Energy's Building Technology Office, capable of performing dynamic simulations, providing detailed energy analysis.

An office test room, to be considered part of a multi-storey building, was consequently modeled. The floor surface was 20 m^2 and the internal height was 3.5 m. The gross surface of the glazed envelope was 7.5 m^2 and it was located on one of the vertical walls, which was assumed as the only thermally

exchanging surface (made of wood cladding/thermal insulation/gypsum plaster with U-Factor = 0.35 W/m^2·K).

Glazing and frame properties for all the windows considered in this study were reported in Table 1. The window-to-wall ratio (WWR) was 60%, whereas the surface ratio between frame and glazed area of the window was 41%. Lateral walls (20 cm thick walls) and horizontal surfaces (floor and ceiling, 30 cm thick, U-Factor = 0.819 W/m^2·K) were shared with other offices, and thus considered adiabatic in their external surface. All possible exposures were considered for the windowed wall.

Table 1. Glazing, frame, and dividers properties. All the cavities between glass panes were considered filled with argon gas. Conductance was calculated excluding surface convection resistance.

Window Type	Glazing Structure	Glass U-Factor (W/m^2·K)	Frame and Divider Conductance (W/m^2·K)	Low-e Coating	Frame Materials
Refurbishment scenario	4/16/4	2.60	7.57	-	Aluminium without thermal break
Standard Compliant scenario	4/16/4/16/4	1.08	3.5	Face 5	Aluminium with thermal break

To better point out the role of the window (and its frame), the envelope properties were considered the same in Bari and Toronto, although their respective climates are significantly different. For "Refurbishment scenario" and "Standard compliant scenario", typical values of window frame conductance were considered, as specified in Table 1. A window with a triple glass pane and a low performing frame was not taken into account, in this work, for two main reasons: first of all, we aimed at excluding the effect of glazing when considering the comparison between the standard compliant window and the one equipped with the innovative aerogel. In fact, glazing might have affected simulations much more than frames, due to the larger surface area involved in heat transfer, compared to frames; second, a window with three panes would be technically incompatible with a thin frame for structural and dimensional reasons.

Two locations were taken into account: Bari (Southern Italy) and Toronto (Canada). Their climate specifications are provided in Table 2, showing the significant differences in terms of "extreme" winter conditions. Figure 4 reports yearly solar radiation available on a vertical plane, in Bari and Toronto. Graphs also show that total radiation is similar in the two locations, due to the similar latitude. This confirms that the radiative contribution does not represent an element of inhomogeneity for the analyses reported hereafter. Consequently, main differences in terms of heat transfer are due to frame conductance, rather than sun irradiance.

Table 2. Climate characteristics of the two locations considered in this work.

City	Latitude [°]	Koppen-Geiger Climate Class	Average Temperature [°C]	Winter Average Temperature [°C]	Winter Average Daily Minimum Temperature [°C]	Winter Average Daily Maximum Temperature [°C]
Toronto	43.70	Dfb	9.85	−3.00	−6.53	2.60
Bari	41.11	Csa	16.10	9.87	6.27	13.57

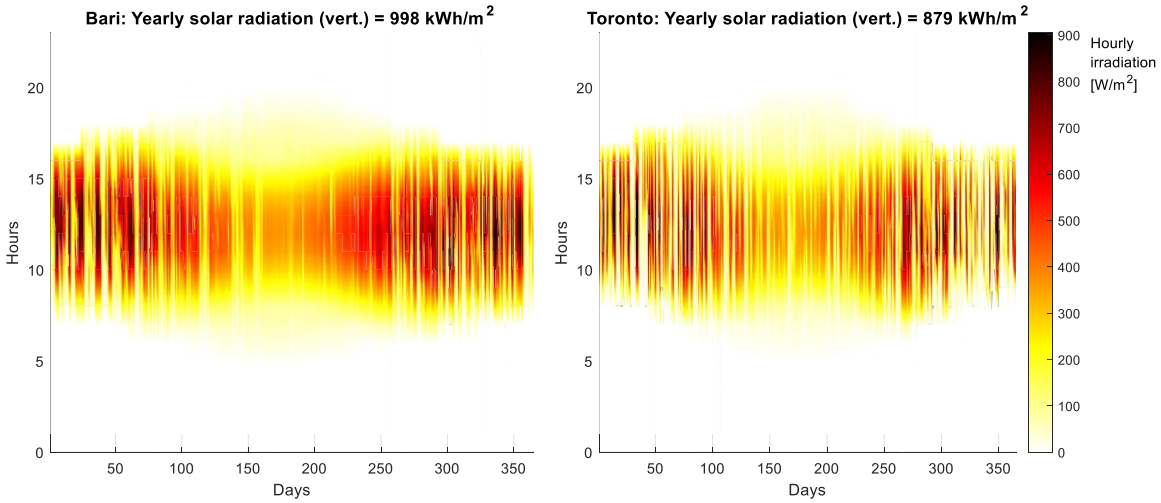

Figure 4. Solar radiation available on vertical planes, in Bari and Toronto.

The heating period was considered according to regulations in force. According to the Italian regulations, Bari falls in a climatic zone in which heating systems work from November 15th to March 31st, whereas in Toronto, heating works from October 1st to May 15th. The cooling period was considered to extend from July 1st to September 30rd both in Bari and Toronto, with average temperatures of 23.1 °C and 19.5 °C, respectively. In the proposed model, EnergyPlus provides heating and cooling energy required to meet the temperature at a set point of 20.5 °C in heating mode and 26 °C in cooling mode. To calculate energy use for heating and cooling with a simplified method an "IdealLoadAirSystem" was used, which gives the thermal energy strictly necessary to achieve the given set-point temperature. Zone ventilation was assumed to be 0.0025 m^3/s, according to ASHRAE 62.1/2013, Table 6.2.2.1. Infiltrations were considered 0.0003 $m^3/s{\cdot}m^2$ of exterior surface area, and an "always on" schedule was applied. Internal gains due to equipment were taken into account to the extent of 5 W/m^2, whereas artificial lighting was considered as 10.66 W/m^2.

3. Results

3.1. FEM Model

Numerical analysis, by means of FEM modeling, was made to investigate the thermal figures of merit of a frame containing granular aerogel, acting as a "thermal break" within an aluminium/wood frame. To obtain intelligible information, in this case, we compared a highly performing frame, containing expanded polystyrene insulator with the new aerogel-insulated window. In this way, ceteris paribus, the only difference in thermal performance were due to the materials properties, rather than surface area, thickness, or distribution. Due to the low thermal conductivity of the aerogel granules, a significant reduction of the U_f was achieved (1.23 $W/m^2{\cdot}K$, using EPS). The value found after the simulation process was 0.66 $W/m^2{\cdot}K$ for the frame and divider conductance. This further comparison demonstrates that one of the most interesting advantages of using aerogel for thermal insulation consists in reducing the thickness of the materials adopted, in the face of significant increases in thermal resistance.

The temperature field of the frame embodying granular aerogel shows the effectiveness of the aerogel "thermal break". In fact, the large number of isothermal lines concentrated within the aerogel "thermal break", in which a thermal variation of about 10 °C is detected in a few centimeters of thickness, demonstrates that the thermal performance of the insulating material used is very good (Figure 5a). This confirms that aerogel can act as an effective thermal barrier at the interface between the two materials that constitute the cross-section of the designed frame (wood and aluminium). As a

comparison, the use of the polystyrene insulation (Figure 5b) clearly shows that the thermal variation between the faces and the distribution of the isothermal lines are much less effective.

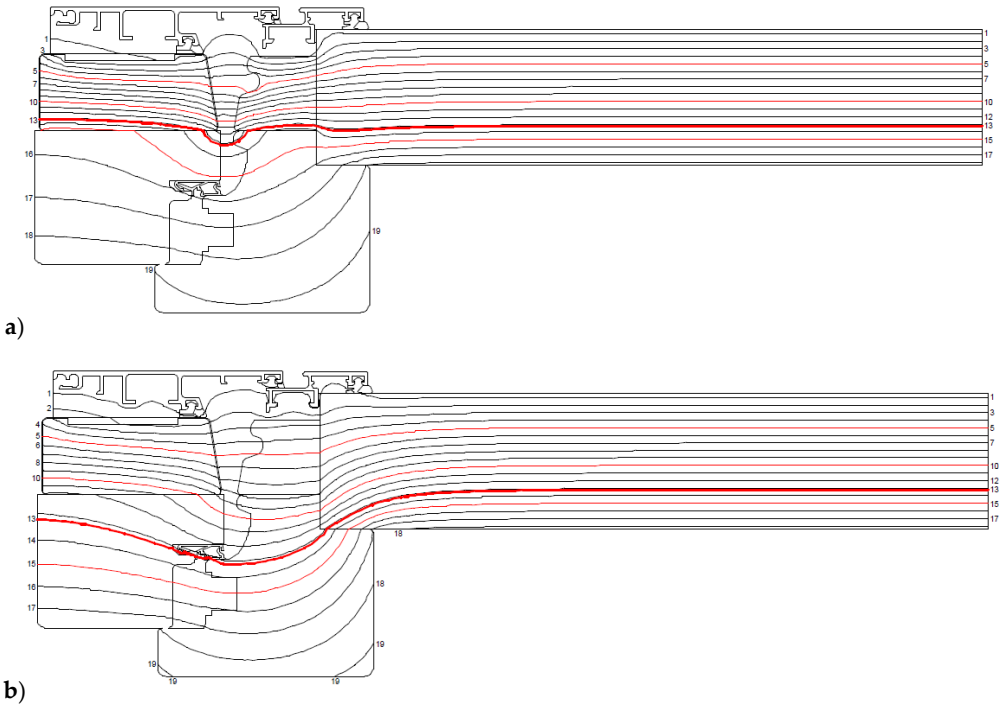

Figure 5. Isothermal lines within the cross section of the newly designed frame with aerogel insulation (**a**) and with expanded polystyrene insulation (**b**). Numbers reported in the figure represent temperatures corresponding to isothermal lines, expressed in °C.

3.2. Energy Consumption

In the subsequent analysis, the energy consumption for heating and cooling was presented in terms of the normalized value per unit floor surface and per year, in order to provide easily comparable results. With reference to heating (Figure 6), in both the cities, maximum heating energy use was observed for the North-facing façade, as expected. The minimum results were found to occur on the Southern façade. On the other hand, intermediate consumptions were observed for the East and West orientations. Predictably, the energy required for heating in winter was higher in the city of Toronto than in Bari. In Toronto, during the heating season, the innovative window, embodying aerogel, allowed an energy saving of 6.9 kWh/m^2·yr on the South exposure, compared to the Refurbishment scenario. This figure reached ~8 kWh/m^2·yr on the East and West exposures. The maximum amount of energy saving reached 12 kWh/m^2·yr on the Northern facade. Nevertheless, the difference in energy saving between the innovative window and the one compliant to regulations was much lower. In fact, the comparison between the newly designed window and the Standard scenario gave the observation that the amount of energy saving strictly due to the superior aerogel thermal performance was ~2 kWh/m^2·yr on the Northern orientation. The relevant change in thermal conductance, among the frame technologies adopted in this study, affects the output of dynamic simulations, generating an offset in energy consumption that may be explained in terms of thermal performance of the window frame, when all the other parameters are kept constant. Such an effect was amplified in Toronto, rather than in Bari, as thermal power is proportional to the temperature difference between the external environment and indoor air.

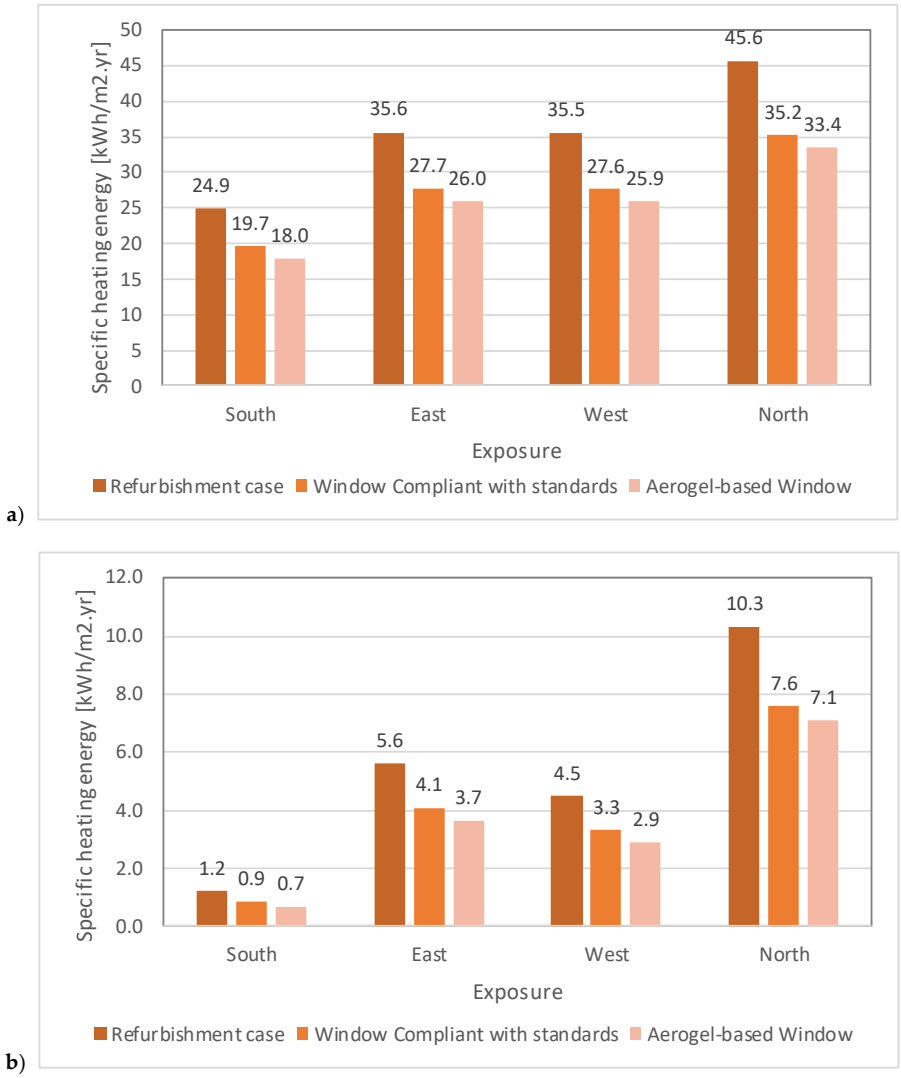

Figure 6. Energy use (kWh/m^2·yr) in Toronto (**a**) and in Bari (**b**), according to exposures and window type.

For this reason, energy saving was lower in Bari, mainly due to its climate conditions, though showing similar tends compared to Toronto: the highest saving during the heating season in Bari was observed assuming the North orientation with reference to the Refurbishment case (3.2 kWh/m^2·yr) and ~2 kWh/m^2·yr for the East and West facades. In Bari, the saving achieved by switching from the compliant window to the aerogel-insulated one was lower than in Toronto (below 1 kWh/m^2·yr); these results are consistent with the considerations exposed above.

The situation was completely reversed between the two locations when the consumption for summer cooling was taken into consideration (Figure 7). In this case, the consumptions of energy for cooling prevailed in Bari, where they were approximately double compared to those observed in Toronto. The façade orientations with higher consumptions were South, East, and West, both in Toronto and Bari. In all cases, the saving achievable by adopting the innovative frame was negligible, whereas the differences observed with respect to the reference window (Refurbishment scenario) were mainly due to the reduction in the incoming radiation through the triple glass with low transmittance. The maximum savings were 4 kWh/m^2·yr in Toronto on the South façade and ~6 kWh/m^2·yr for the same orientation in Bari. In both locations, cooling energy was slightly higher in the aerogel-base window, compared to the one compliant with standards. As the method used in dynamic simulations using the Energyplus platform is deterministic in nature, the observed differences can only be explained in terms

of differences in the thermal conductance of the window frame. Consequently, it may be deduced that the lower thermal transmittance of the window containing aerogel, during the summer season, reduces heat exchanges during the night time, thus limiting the beneficial removal of cooling loads associated with sensible thermal power due to equipment, lighting density, persons, and heat transfer through the opaque and transparent envelopes.

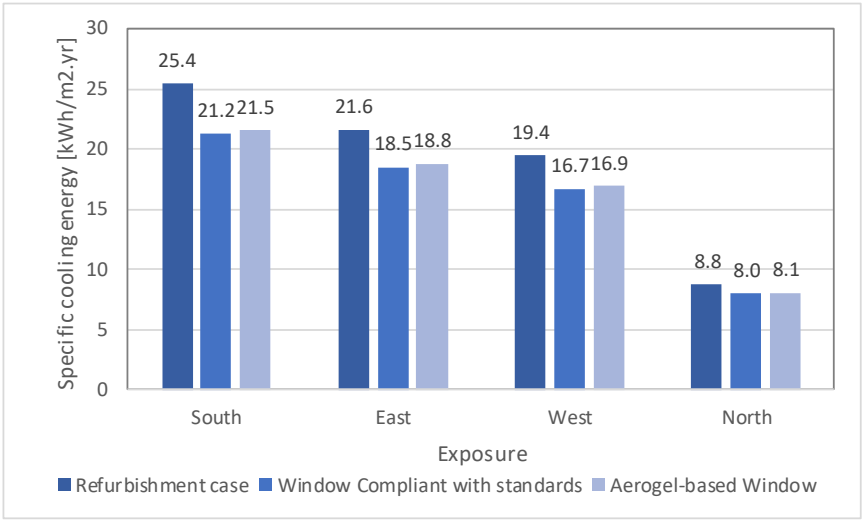

a)

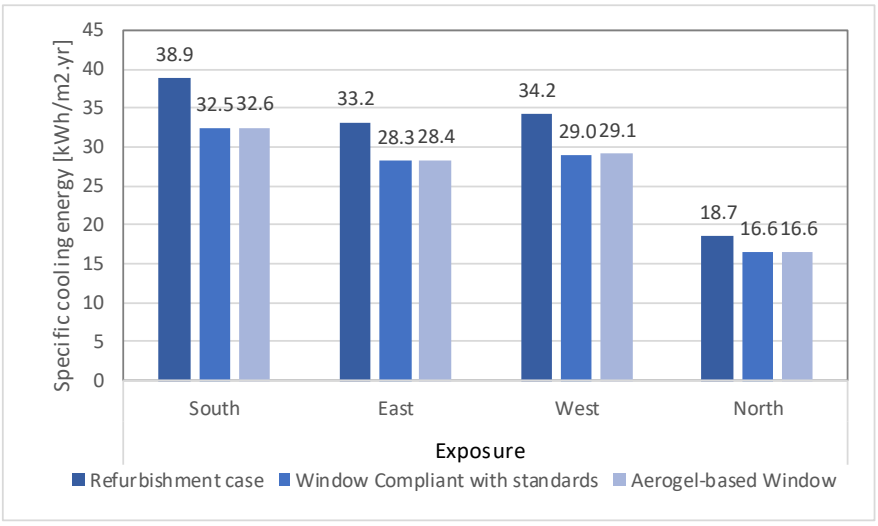

b)

Figure 7. Cooling energy consumptions (kWh/m^2·yr) in Toronto (**a**) and in Bari (**b**), according to exposures and window type.

Reduction in the frame U-factor might improve the thermal performance of windows and influence the indoor temperatures in cold climates, as verified in Toronto. The analyses carried out clearly showed the extent to which the location may influence the achievable energy performance, especially in terms of energy saving. The highest saving (~27%) for heating consumption was attained in Toronto on the North-facing exposure, comparing the performance obtained using the innovative window with those reported for the Refurbishment scenario, and 6% comparing it with a Standard compliant scenario. In Bari, the results were equally high in percentage terms, reaching 27% and 7%, respectively, with reference to the winter season and energy use for heating, although these results were not so significant in absolute terms.

3.3. Frame Temperatures

The hourly surface frame temperature inside the room was reported in Figure 8 on an annual basis, taking into account only the facades exposed to North, as they were those in which the innovative frame showed the best performance. It is clear that during the entire winter season, in Toronto, the strongly insulating properties of the frame of the innovative window might guarantee a rather sharp increase in temperature (up to 5 °C) compared to the other two frame technologies. During the summer season, the frame temperature was lower than in the frames adopted for the other scenarios. In Bari, the performance difference was barely noticeable as well, because the different climatic conditions did not emphasize the difference in thermal performances. Regardless, also in this case, frame temperature was higher in winter and lower in summer, confirming the behavior observed in Toronto. In Bari, the maximum temperature differences observed in January were 4.1 °C and 6.19 °C, respectively, compared to the Standard compliant scenario frame and the Refurbishment scenario. In June, the highest temperature differences were 3.35 °C and 7.44 °C, in the cooling season, taking into account the same reference scenarios as above. As shown in Table 1, the value of the frame conductance is halved when switching from the Refurbishment scenario to the Standard Compliant scenario, but is further reduced by a factor of 5.5, by switching the latter to the innovative, aerogel-based frame. This justifies the different data of the internal temperature in the months from December to April (Figure 8a), in which we take better advantage of the greater level of thermal insulation offered by the best performing frame in the cold seasons, in the climate conditions of Toronto.

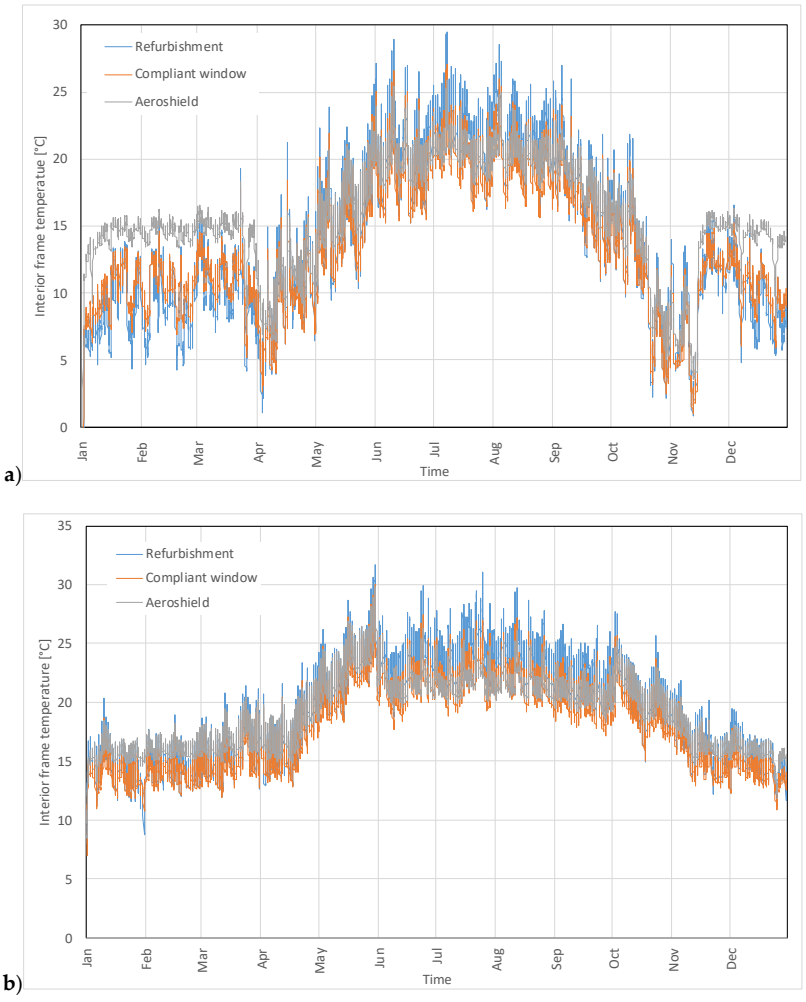

Figure 8. Frame surface temperature for North exposure, plotted with reference to one-year time, in Toronto (**a**) and Bari (**b**).

3.4. North-Facades in Toronto

Starting from these remarks, further analyses were carried out to compare performances due to different values of Window-to-Wall Ratios (WWRs) of North-facing walls in Toronto. Three different values of Window-to-Wall Ratio were considered to take into account the effect of window size on the North-facing exposure as well as the effect of the frame surface, in each case. The window used in previous simulations was then assumed as the "intermediate" case window. Two more sizes were added: a "small" and a "large" window, as suitable terms of comparison. For each case, the Frame-to-Glazing Ratio (FGR) was also calculated, expressing the ratio between the frame surface and the glazing surface, in percentage terms (Figure 9).

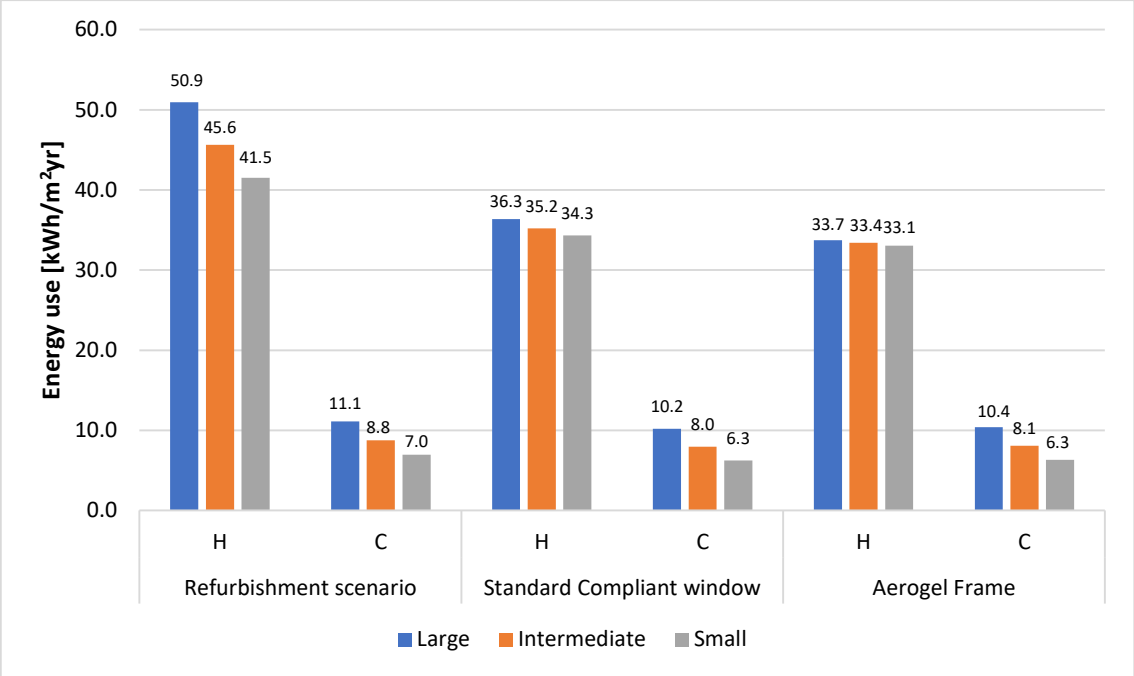

Figure 9. Energy use for heating and cooling using three different window sizes on the North-facing exposure, in Toronto. (H= Heating, C= Cooling).

When the aerogel window was compared with the Refurbishment scenario, the "large" window (WWR = 100%) showed the highest saving (17 kWh/m^2·yr), passing from 51 to 34 kWh/m^2·yr yearly consumption for heating. This figure dropped to 12 kWh/m^2·yr when the intermediate window was considered (WWR = 60%) and to 8.4 kWh/m^2·yr in the small window (WWR = 43%).

When the aerogel window was compared with the Standard compliant scenario, the highest contribution to energy saving due to the aerogel frame only was observed in the large window (3 kWh/m^2·yr). The better performance of this case was due to the greater contribution of the frame on the overall façade surface, expressed by the higher FGR (46%), compared to the "intermediate" and "small" window, with lower FGRs (41% and 39%, respectively).

The effect of FGR on energy consumption, for all the window sizes and frame technologies, was taken into account by normalizing the overall yearly energy consumption (for cooling and heating) by the actual frame surface area (Table 3). The table shows that the increase of glazed area has a larger impact than the frame technology adopted, implying larger consumption, in all the cases investigated. Anyway, lower energy consumption occurred in the aerogel-insulated windows, although the standard compliant window and aerogel-insulated window show almost comparable results. The lowest normalized consumption (about 5%), for the aerogel-insulated window, compared to the standard compliant window, was obtained when the WWR was set to 43%.

Table 3. Yearly energy consumption normalized to frame surface area.

Window Size	WWR (%)	FGR (%)	Window Surface Area (m^2)	Frame Surface Area (m^2)	Normalized Yearly Energy Consumption ($kWh/m^2 \cdot yr$)		
					Refurbishment	Standard-Compliant	Aerogel-Insulated
Small	43	39	5.3	2.0	221.6	166.3	157.5
Intermediate	60	42	7.3	3.0	362.6	287.8	276.5
Large	100	46	12.2	5.6	484.7	405.7	393.8

4. Discussion

The results obtained in this study showed that even when reducing U_f from 3.5 to 0.66 $W/m^2 \cdot K$, by means of the best available technologies, the achievable benefits in terms of energy saving were significant only on North-facing walls, and in more extreme cold climates. Clearly, the transparent component of the window plays a major role in determining the final result, as the comparison between the "refurbishment" and the "standard compliant" cases showed, but FGR values proved that frame may be equally significant when smaller glass panes are used. Thus, proper economic considerations might be useful to improve understanding of the practical advantages of such technologies. According to Koebel et al. (2012), the price of aerogel could drop below 1500 USD/m^3 by 2020. In line with this, other studies reveal that the cost of a meter cube of aerogel will achieve 50% cost reduction in production within the next few years and will decrease to 660 USD/m^3 by 2050 [13,35]. Assuming the latter value for the volume cost of granular aerogel, less than 20 USD would be required to fabricate the super-insulated aerogel-based window at the basis of this study, considering that the aerogel volume in the frame would be ~0.011 m^3. Furthermore, the real challenge for a significant cost reduction for the aerogel does not seem to come from mass production using the supercritical drying process (the process that is currently used by all the manufactures of aerogel products), but from the definition of new methods for evacuating the liquid component of the gel. In particular, the ambient drying process has already shown some preliminary advantages depicted over a decade ago by Bhagat et al. in 2007 [36]. More recently, Koebel et al. [37] and Wu et al. [38] explored successful ways to fabricate large quantities of aerogel using ambient-dried silica aerogel. These methods have also been applied by Berardi and Zaidi [6], who in 2019 presented a new ambient pressure drying aerogel blanket.

5. Conclusions

The results presented in this paper constitute an interesting premise for further experimental investigations on the here proposed innovative window. The aerogel-based window outperformed both the obsolete window adopted for a "Refurbishment scenario", and the highly performing "Standard compliant" one, showing reduction of energy uses by 27% and 6%, respectively.

The overall effect on energy use due to the improvement of the frame thermal resistance is limited superiorly by its surface, compared to that of the glazed component, generally lower than 50%. In the present work, it has been proven that the conductance of the frame can be much lower compared with that of a highly performing triple glass.

This work has shown the effectiveness of significantly lowering the frame conductance, opening the way to further investigations taking into account both energy saving and the increase of cost due to the use of super-insulating materials, inside the frame.

Author Contributions: Conceptualization, A.C.; methodology, A.C.; writing—original draft preparation, A.C.; writing—review and editing, U.A., U.B., A.C., V.D.C., S.L., F.M., and C.R. All authors have read and agreed to the published version of the manuscript.

Funding: This research was partially funded by the Action Co-founded by Cohesion and Development Fund 2007–2013 – APQ Research Puglia Region "Regional programme supporting smart specialization and social and environmental sustainability – Future in Research".

Acknowledgments: Antonio Ferrara and the technical team from DCS Group s.r.l. are kindly acknowledged for their support during the fabrication of the aerogel-based window; Cabot Company is gratefully acknowledged for providing the granular aerogel used for the fabrication of the new window frame prototype.

Conflicts of Interest: The authors declare no conflict of interest.

References

1. Parliament, E. Directive (EU) 2018/844 of the European Parliament and of the Council of 30 May 2018 Amending Directive 2010/31/EU on the Energy Performance of Buildings and Directive 2012/27/EU on Energy Efficiency. Available online: https://eur-lex.europa.eu/eli/dir/2018/844/oj (accessed on 1 February 2020).
2. Wen, R.T.; Arvizu, M.A.; Niklasson, G.A.; Granqvist, C.G. Electrochromics for energy efficient buildings: Towards long-term durability and materials rejuvenation. *Surf. Coat. Technol.* **2015**, *278*, 121–125. [CrossRef]
3. Eperon, G.E.; Burlakov, V.M.; Goriely, A.; Snaith, H.J. Neutral color semitransparent microstructured perovskite solar cells. *ACS Nano* **2014**, *8*, 591–598. [CrossRef] [PubMed]
4. Cannavale, A.; Ierardi, L.; Hörantner, M.; Eperon, G.E.; Snaith, H.J.; Ayr, U.; Martellotta, F. Improving energy and visual performance in offices using building integrated perovskite-based solar cells: A case study in Southern Italy. *Appl. Energy* **2017**, *205*, 834–846. [CrossRef]
5. Jelle, B.P. Traditional, state-of-the-art and future thermal building insulation materials and solutions - Properties, requirements and possibilities. *Energy Build.* **2011**, *43*, 2549–2563. [CrossRef]
6. Berardi, U. Characterization of commercial aerogel-enhanced blankets obtained with supercritical drying and of a new ambient pressure drying blanket. *Energy Build.* **2019**, *198*, 542–552. [CrossRef]
7. De Matteis, V.; Cannavale, A.; Martellotta, F.; Rinaldi, R.; Calcagnile, P.; Ferrari, F.; Ayr, U.; Fiorito, F. Nano-encapsulation of phase change materials: From design to thermal performance, simulations and toxicological assessment. *Energy Build.* **2019**, *188*, 1–11. [CrossRef]
8. Ascione, F.; Bianco, N.; De Masi, R.F.; de' Rossi, F.; Vanoli, G.P. Energy refurbishment of existing buildings through the use of phase change materials: Energy savings and indoor comfort in the cooling season. *Appl. Energy* **2014**, *113*, 990–1007. [CrossRef]
9. Buratti, C.; Belloni, E.; Palladino, D. Evolutive Housing System: Refurbishment with new technologies and unsteady simulations of energy performance. *Energy Build.* **2014**, *74*, 173–181. [CrossRef]
10. Bahaj, A.S.; James, P.A.B.; Jentsch, M.F. Potential of emerging glazing technologies for highly glazed buildings in hot arid climates. *Energy Build.* **2008**, *40*, 720–731. [CrossRef]
11. Jelle, B.P.; Baetens, R.; Gustavsen, A. Aerogel Insulation for Building Applications. In *Sol-Gel Handbook*; Wiley-VCH Verlag GmbH & Co. KGaA: Weinheim, Germany, 2015; Volume 3, pp. 1385–1412.
12. Walker, R.; Pavía, S. Thermal performance of a selection of insulation materials suitable for historic buildings. *Build. Environ.* **2015**, *94*, 155–165. [CrossRef]
13. Cuce, E.; Cuce, P.M.; Wood, C.J.; Riffat, S.B. Toward aerogel based thermal superinsulation in buildings: A comprehensive review. *Renew. Sustain. Energy Rev.* **2014**, *34*, 273–299. [CrossRef]
14. Berardi, U. Aerogel-enhanced insulation for building applications. In *Nanotechnology in Eco-efficient Construction (Second Edition), Materials, Processes and Applications*; Woodhead Publishing: Cambridge, UK, 2018; pp. 395–416.
15. Parameshwaran, R.; Kalaiselvam, S. *Nano and Biotech Based Materials for Energy Building Efficiency*; Pacheco Torgal, F., Buratti, C., Kalaiselvam, S., Granqvist, C.-G., Ivanov, V., Eds.; Springer International Publishing: Cham, Switzerland, 2016; pp. 215–243; ISBN 978-3-319-27505-5.
16. Buratti, C.; Moretti, E.; Belloni, E. Aerogel plasters for building energy efficiency. In *Nano and Biotech Based Materials for Energy Building Efficiency*; Springer Nature: Cham, Switzerland, 2016; pp. 17–40.
17. Ebert, H.-P. Thermal Properties of Aerogels. In *Aerogels Handbook*; Springer Nature: Cham, Switzerland, 2011; pp. 537–564.
18. Berardi, U. The development of a monolithic aerogel glazed window for an energy retrofitting project. *Appl. Energy* **2015**, *154*, 603–615. [CrossRef]
19. Neugebauer, A.; Chen, K.; Tang, A.; Allgeier, A.; Glicksman, L.R.; Gibson, L.J. Thermal conductivity and characterization of compacted, granular silica aerogel. *Energy Build.* **2014**, *79*, 47–57. [CrossRef]
20. Ihara, T.; Jelle, B.P.; Gao, T.; Gustavsen, A. Aerogel granule aging driven by moisture and solar radiation. *Energy Build.* **2015**, *103*, 238–248. [CrossRef]
21. Hoseini, A.; McCague, C.; Andisheh-Tadbir, M.; Bahrami, M. Aerogel blankets: From mathematical modeling to material characterization and experimental analysis. *Int. J. Heat Mass Transf.* **2016**, *93*, 1124–1131. [CrossRef]

22. Cuce, E.; Cuce, P.M. The impact of internal aerogel retrofitting on the thermal bridges of residential buildings: An experimental and statistical research. *Energy Build.* **2016**, *116*, 449–454. [CrossRef]
23. Ng, S.; Jelle, B.P.; Sandberg, L.I.C.; Gao, T.; Wallevik, Ó.H. Experimental investigations of aerogel-incorporated ultra-high performance concrete. *Constr. Build. Mater.* **2015**, *77*, 307–316. [CrossRef]
24. Gao, T.; Jelle, B.P.; Gustavsen, A.; He, J. Lightweight and thermally insulating aerogel glass materials. *Appl. Phys. A Mater. Sci. Process.* **2014**, *117*, 799–808. [CrossRef]
25. Berardi, U. Development of glazing systems with silica aerogel. *Energy Procedia* **2015**, *78*, 394–399. [CrossRef]
26. Jelle, B.P.; Hynd, A.; Gustavsen, A.; Arasteh, D.; Goudey, H.; Hart, R. Fenestration of today and tomorrow: A state-of-the-art review and future research opportunities. *Sol. Energy Mater. Sol. Cells* **2012**, *96*, 1–28. [CrossRef]
27. Dowson, M.; Harrison, D.; Craig, S.; Gill, Z. Improving the Thermal Performance of Single Glazed Windows using Translucent Granular Aerogel. *Int. J. Sustain. Eng.* **2011**, *4*, 266–280. [CrossRef]
28. Huang, Y.; Niu, J. Application of super-insulating translucent silica aerogel glazing system on commercial building envelope of humid subtropical climates e Impact on space cooling load. *Energy* **2015**, *83*, 316–325. [CrossRef]
29. Gao, T.; Ihara, T.; Grynning, S.; Petter, B.; Gunnarshaug, A. Perspective of aerogel glazings in energy efficient buildings. *Build. Environ.* **2016**, *95*, 405–413. [CrossRef]
30. Buratti, C.; Moretti, E. Experimental performance evaluation of aerogel glazing systems. *Appl. Energy* **2012**, *97*, 430–437. [CrossRef]
31. Buratti, C.; Moretti, E. Glazing systems with silica aerogel for energy savings in buildings. *Appl. Energy* **2012**, *98*, 396–403. [CrossRef]
32. Valachova, D.; Zdrazilova, N.; Panovec, V.; Skotnicova, I. Using of aerogel to improve thermal insulating properties of windows. *Civ. Environ. Eng.* **2018**, *14*, 2–11. [CrossRef]
33. EnergyPlus 8.9, Building Technologies Program, National Renewable Energy Laboratory (NREL). Available online: https://energyplus.net/ (accessed on 1 July 2019).
34. ISO 10077-2:2017 - Thermal Performance of Windows, Doors and Shutters—Calculation of Thermal Transmittance Numerical Method for Frames; Standards Norway. 2017. Available online: https://www.iso.org/standard/64995.html (accessed on 1 July 2019).
35. Koebel, M.; Rigacci, A.; Achard, P. Aerogel-based thermal superinsulation: An overview. *J. Sol-Gel Sci. Technol.* **2012**, *3*, 315–339. [CrossRef]
36. Bhagat, S.D.; Kim, Y.-H.; Moon, M.-J.; Ahn, Y.-S.; Yeo, J.-G. A cost-effective and fast synthesis of nanoporous SiO_2 aerogel powders using water-glass via ambient pressure drying route. *Solid State Sci.* **2007**, *9*, 628–635. [CrossRef]
37. Koebel, M.M.; Huber, L.; Zhao, S.; Malfait, W.J. Breakthroughs in cost-effective, scalable production of superinsulating, ambient-dried silica aerogel and sili-ca-biopolymer hybrid aerogels: From laboratory to pilot scale. *J. Sol-Gel Sci. Technol.* **2016**, *79*, 308–318. [CrossRef]
38. Wu, X.; Fan, M.; Mclaughlin, J.F.; Shen, X.; Tan, G. A novel low-cost method of silica aerogel fabrication using fly ash and trona ore with ambient pressure drying technique. *Powder Technol.* **2018**, *323*, 310–322. [CrossRef]